The Cryosphere Discuss., 5, 3129–3173, 2011
www.the-cryosphere-discuss.net/5/3129/2011/
doi:10.5194/tcd-5-3129-2011

The Cryosphere Discussions

Estimating ice phenology on large northern lakes from AMSR-E: algorithm development and application to Great Bear Lake and Great Slave Lake, Canada

K.-K. Kang[1,2], C. R. Duguay[1,2], and S. E. L. Howell[3]

[1]Interdisciplinary Centre on Climate Change (IC3), University of Waterloo, Waterloo, Ontario N2L 3G1, Canada
[2]Department of Geography and Environmental Management, University of Waterloo, Waterloo, Ontario N2L 3G1, Canada
[3]Climate Research Division, Environment Canada, 4905 Dufferin Street, Toronto, Ontario M3H 5T4, Canada

Received: 9 October 2011 – Accepted: 29 October 2011 – Published: 14 November 2011

Correspondence to: K.-K. Kang (kkkang@uwaterloo.ca)

Published by Copernicus Publications on behalf of the European Geosciences Union.

Abstract

Time series of brightness temperatures (T_B) from the Advanced Microwave Scanning Radiometer-Earth Observing System (AMSR-E) are examined to determine ice phenological parameters on the two largest lakes of northern Canada: Great Bear Lake (GBL) and Great Slave Lake (GSL). T_B measurements from the 18.7, 23.8, 36.5, and 89.0 GHz channels (H- and V- polarization) are compared to assess their potential for detecting freeze-onset/melt-onset and ice-on/ice-off dates on both lakes. The 18.7 GHz (H-pol) channel is found to be the most suitable for estimating these ice dates as well as the duration of the ice cover and ice-free seasons. A new algorithm is proposed using this channel and applied to map all ice phenological parameters on GBL and GSL over seven ice seasons (2002–2009). Analysis of the spatio-temporal patterns of each parameter at the pixel level reveals that: (1) both freeze-onset and ice-on dates occur on average about one week earlier on GBL than on GSL (Day of Year (DY) 318 and 333 for GBL; DY 328 and 343 for GSL); (2) the freeze-up process or freeze duration (freeze-onset to ice-on) takes a slightly longer amount of time on GBL than on GSL (about 1 week on average); (3) melt-onset and ice-off dates occur on average one week and approximately four weeks later, respectively, on GBL (DY 143 and 183 for GBL; DY 135 and 157 for GSL); (4) the break-up process or melt duration (melt-onset to ice-off) lasts on average about three weeks longer on GBL; and (5) ice cover duration estimated from each individual pixel is on average about three weeks longer on GBL compared to its more southern counterpart, GSL. A cross-comparison of dates for several ice phenological parameters derived from other satellite remote sensing products (e.g. NOAA Interactive Multisensor Snow and Ice Mapping System (IMS), QuikSCAT, and Canadian Ice Service Database) show that, despite its relatively coarse spatial resolution, AMSR-E 18.7 GHz provides a viable means for monitoring of ice phenology on large northern lakes.

TCD

5, 3129–3173, 2011

1 Introduction

Lake ice cover is an important component of the terrestrial cryosphere for several months of the year in high-latitude regions (Duguay et al., 2003). Lake ice is not only a sensitive indicator of climate variability and change, but it also plays a significant role in energy and water balance at local and regional scales. The presence of an ice cover alters lake-atmosphere exchanges (Duguay et al., 2006; Brown and Duguay, 2010). When energy movement occurs during temperature change, heat transfer (thermodynamics) influences ice thickening as well as the timing and duration of freeze-up and break-up processes, which is referred to as ice phenology (Jeffries and Morris, 2007). Lake ice phenology, which encompasses freeze-onset/melt-onset, ice-on/ice-off dates, and ice cover duration, is largely influenced by air temperature changes and is therefore a robust indicator of climate conditions (e.g. Bonsal et al., 2006; Duguay et al., 2006; Kouraev et al., 2007a; Latifovic and Pouliot, 2007; Schertzer et al., 2008; Howell et al., 2009).

The analysis of historical trends (1846–1995) in in situ lake and river ice phenology has provided evidence of later freeze-up (ice-on) and earlier break-up (ice-off) dates at the northern hemispheric scale (Magnuson et al., 2000; Brown and Duguay, 2010). In Canada, from 1951 to 2000, trends towards earlier ice-off dates have been observed for many lakes, but ice-on dates have shown few significant trends over the same period (Duguay et al., 2006). The observed changes in Canada's lake ice cover have also been found to be influenced by large-scale atmospheric forcings (Bonsal et al., 2006). Canada's government-funded historical ground-based observational network has provided much of the evidence for the documented changes for most of the 20th century and for establishing links with variations in atmospheric teleconnection indices, notably Pacific oscillation patterns such as Pacific North American Pattern (PNA) and Pacific Decadal Oscillation (PDO). Unfortunately, the Canadian ground-based lake ice network has been eroded to the point where it can no longer provide the quantity of observations necessary for climate monitoring across the country. Satellite remote

TCD
5, 3129–3173, 2011

sensing is the most logical means for establishing a global observational network as the diminishing trend in the ground-based lake ice network seen in Canada has been mimicked in many other countries of the Northern Hemisphere (IGOS, 2007).

From a satellite remote sensing perspective, dates associated with estimating the freeze-up process (i.e. onset of freeze until a complete sheet of ice is formed) in autumn and early winter are particularly difficult to determine using optical satellite sensors such as the Moderate Resolution Imaging Spectroradiometer (MODIS) and the Advanced Very High Resolution Radiometer (AVHRR) on high-latitude lakes due to long periods of obscurity and extensive cloud cover (Maslanik et al., 1987; Jeffries et al., 2005b; Latifovic and Pouliot, 2007). QuikSCAT has been used successfully to derive and map freeze-onset, melt-onset and ice-off dates on Great Bear Lake (GBL) and GSL (Howell et al., 2009). Unfortunately, QuikSCAT data are no longer available for lake ice monitoring on large lakes since its nominal mission ended on 23 November 2009, due to antenna spin rate degradation. Previous investigations have shown the utility of observing lake ice phenological parameters through the visual interpretation of brightness temperature (T_B) changes from the Scanning Multichannel Microwave Radiometer (SMMR) at 37 GHz (Barry and Maslanik, 1993) and the Special Sensor Microwave/Imager (SSM/I) at 85 GHz (Walker et al., 1993, 2000) on Great Slave Lake (GSL), one of the two lakes of this study, but identifying spatial variability in these parameters is difficult due to their coarse resolution (~25 km). In a recent study, SSM/I has been used in combination with radar altimetry to determine automatically ice phenological events on Lake Baikal (Kouraev et al., 2007a).

Measurements from the Advanced Microwave Scanning Radiometer-Earth Observing System (AMSR-E) that offer improved spatial resolution have yet to be assessed for monitoring ice phenology. The objectives of this paper are to (i) evaluate the utility of AMSR-E T_B measurements of estimating lake ice phenology, (ii) develop a comprehensive algorithm for mapping lake ice phenological parameters, and (iii) apply the algorithm over both GBL and GSL to investigate the spatio-temporal variability of each lakes ice phonology from 2002 to 2009.

2 Background

2.1 Passive microwave radiometry of lake ice

The discrimination of ice cover characteristics from passive microwave T_B measurements requires a good knowledge of the radiometric properties of ice in nature (Kouraev et al., 2007a). In contrast to the high-loss characteristics of sea ice (due to salinity), one of the major microwave characteristics of pure freshwater ice is its low-loss transmission behavior (Ulaby et al., 1986). The brightness temperature (T_B) at passive microwave frequencies is defined as the product of the emissivity (ε) and physical temperature (T_{kin}) of the medium:

$$T_B = \varepsilon T_{kin} \quad (1)$$

Passive microwave systems can measure, regardless of cloud coverage and darkness, naturally emitted radiation through T_B. Since emissivity ranges between 0 and 1, the T_B is lower than the kinetic temperature of the medium. The large change in emissivity from open water ($\varepsilon = 0.443$–0.504 at 24 GHz) to ice covered conditions ($\varepsilon = 0.858$–0.908 at 24 GHz) (Hewison and English, 1999; Hewison, 2001) makes the determination of the timing of ice formation and decay on large, deep lakes, feasible from T_B measurements. The emissivity of ice, and therefore T_B, further increases from its initial formation as the effect of the radiometrically cold water under the ice surface decreases with ice thickening (Kang et al., 2010).

2.2 Definitions of ice phenological parameters

The definitions of freeze-up and break-up are opposite: the former describes the time period between the beginning of ice formation and the formation of a complete sheet of ice, while the latter describes the time period between the onset of spring melt and the complete disappearance of ice from the lake surface. Since the algorithm presented herein operates on a pixel-by-pixel basis and is applied over entire lake surfaces, it is

TCD
5, 3129–3173, 2011

important to provide clear definitions of the ice phenological parameters as they relate to individual pixels and over whole lakes (or lake sections) (Table 1). At the level of the pixel, the freeze-up period encompasses freeze onset (FO), ice-on and freeze duration (FD), while the break-up period comprises melt onset (MO), ice off and melt duration (MD). The period between ice-on and ice-off covers an ice season and is referred to as ice cover duration (ICDp; p for pixel). At the lake or lake section level (third column of Table 1), complete freeze over (CFO), water clear of ice (WCI) and ice cover duration (ICDe; e for entire lake or lake sections as to avoid land contamination in some AMSR-E T_B measurements) are the terms used from here onward. CFO corresponds to the date when all pixels within the lake or lake section have become ice-covered (i.e. all flagged with having ice-on). WCI corresponds to the date when all pixels have become ice-free (i.e. all flagged with having ice-off). While ICDp is calculated for each individual pixel from dates of ice-on to ice-off, ICDe is determined as the number of days between CFO and WCI within an ice season.

3 Study area

GBL and GSL are two of the largest freshwater lakes in the world. Located in the Mackenzie River Basin (MRB) they fall within two physiographic regions of Canada's Northwest Territories (NWT): the Precambrian Shield and the Interior Plains (Fig. 1). The eastern parts of both lakes are situated in the Precambrian Shield. Its undulating topography with bedrock outcrops causes the formation of rounded hills and valleys. The high topography of the western Cordillera and low relief of the central and eastern parts of the Mackenzie Basin strongly influence the regional climate (e.g. atmospheric circulation pattern and the advective heat and moisture fluxes) (Woo et al., 2008). Most of GBL and the western/central parts of GSL are located in the flat-lying Interior Plains and underlain by thick glacial, fluvial, and lacustrine deposits; in addition, the Plains are dotted with numerous wetlands and lakes (Woo et al., 2008). GBL and GSL lie between 60° to 67° N and between 109° to 126° W (Fig. 1), and have surface areas (average

TCD
5, 3129–3173, 2011

Title Page
Abstract | Introduction
Conclusions | References
Tables | Figures
◄ | ►
◄ | ►
Back | Close
Full Screen / Esc
Printer-friendly Version
Interactive Discussion

depths) of 31.3×10^3 km^2 (76 m) and 28.6×10^3 km^2 (88 m), respectively (Rouse et al., 2008a; Woo et al., 2008).

The northern extent of GBL is intersected by the Arctic Circle (66.5° N) and hence influenced by colder temperatures than its more southern counterpart (Rouse et al., 2008b). From 2002 to 2009, the period of analysis of this study, the average air temperature recorded at the Deline weather station (65°12′ N, 123°26′ W), near the western shore of GBL, ranged between −25.4 °C and −20.6 °C (winter) and from 10.0 °C to 12.1 °C (summer) with 20.2 cm of average annual snowfall (Table 2). For GBL, complete water turnover occurs at least in some parts of the lake and no break-up occurs until early July (Rouse et al., 2008a).

GSL is part of the north-flowing river system in the Mackenzie Basin (Rouse et al., 2008b). Situated at a more southern location, the mean air temperature in the GSL area is generally warmer than that of GBL, and therefore GSL presents a longer open-water period by about four to six weeks when compared to GBL (Rouse et al., 2008b; Schertzer et al., 2008). GSL is ice-free from the beginning of June until mid- to late-December; however, the ice conditions vary significantly from year to year on this lake (Blanken et al., 2008). The high spatiotemporal variability in air temperature and wind speed over GSL influences the surface water temperature and lake heat flux (Rouse et al., 2008b; Schertzer et al., 2008). From 2002 to 2009, the mean air temperature in winter ranged from −23.8 °C to −15.9 °C and between 13.6 °C and 15.9 °C in summer, with 20.7 cm of average annual snowfall (Table 2). Spring and autumn temperatures, which mark the beginning of the break-up and freeze-up periods, respectively, in the GSL region (−9.5 °C to −1.0 °C; −2.9 °C to 0.1 °C) are higher than near GBL (−11.7 °C to −6.0 °C; −6.9 °C to −3.1 °C) due to the latitudinal difference between the two lakes.

4 Data

Two data sets were used in this study. Primary data correspond to those utilized to examine the sensitivity of passive microwave T_B measurements at various frequencies and to develop the ice phenological algorithm. They consist of meteorological station (air temperature) and AMSR-E data. The secondary, auxiliary, data correspond to ice products or images from other sources. They are used for cross-comparison with the AMSR-E derived ice phenological parameters.

4.1 Primary data

4.1.1 AMSR-E

AMSR-E T_B data were obtained for the period 2002–2009. AMSR-E (fixed incident angle: 54.8 degree) is a conically scanning, twelve-channel passive microwave radiometer system, measuring horizontally and vertically polarized microwave radiation from 6.9 GHz to 89.0 GHz (Kelly, 2009). The instantaneous field-of-view (IFOV) for each channel varies from 76 by 44 km at 6.9 GHz to 6 by 4 km at 89.0 GHz, and the sampling interval of each channel is 10 km (5 km sampling interval in 89.0 GHz). In this study, the AMSR-E/Aqua L2A global swath spatially raw brightness temperature product (AE_L2A) was used.

T_B at 18.7, 23.8, and 36.5 GHz AMSR-E observations for each day falling within a $5.1' \times 5.1'$ grid for both descending and ascending overpasses were averaged over the areas of interest, within the central sections of GBL (66° N, 120°30′ W) and GSL (61°19.8′ N, 115° W and 61°41.8′ N, 113°49.5′ W) (Fig. 1). The 6.9 GHz and 10.7 GHz channels were not considered, as they are more subject to land contamination from lakeshores due to their larger footprint. The divide-and-conquer method for a Delaunay triangulation and inverse distance weighted (IDW) linear interpolation were applied to the L2A data because the T_Bs in ascending and descending modes did not have matching geographic positions over GBL and GSL due to different orbit overpasses. The sampling intervals at all frequency bands are spaced every 10 km (5 km at 89.0 GHz) along and across track in AMSR-E L2A products (Kelly, 2009). Therefore, we chose 10 km grid spacing for the linear interpolation, except for 89 GHz which was at 5 km.

4.1.2 Meteorological station data

Meteorological data from the National Climate Data and Information Archive of Environment Canada (http://climate.weatheroffice.ec.gc.ca/climateData/canada_e.html) were acquired from three stations located in the vicinity of GBL and GSL. The stations selected include Deline (YWJ, 65°12′ N, 123°26′ W) to provide climate information on GBL, and Yellowknife (YZF, 62°27.6′ N, 114°26.4′ W) and Hay River (YHY, 60°50.4′ N, 115°46.8′ W) to characterize the climate in the GSL area (Fig. 1). Time series of maximum and mean air temperatures from 2002 to 2009 were used for comparison with AMSR-E T_B measurements as supporting data for the development of the ice phenological algorithm.

4.2 Auxiliary data

Auxiliary data used for cross-comparison with AMSR-E derived ice phenological parameters consisted of NOAA/IMS ice products, weekly ice observations from the Canadian Ice Service (CIS) during freeze-up and break-up period, and Moderate Resolution Imaging Spectroradiometer (MODIS) images acquired during the break-up period (not examined during freeze-up due to polar darkness). FO, MO, and ice-off dates derived from the QuikSCAT SIR eggs product at the pixel scale by Howell et al. (2009) are compared with the same ice phenological parameters derived from AMSR-E for the period 2002–2006.

The NOAA Interactive Multisensor Snow and Ice Mapping System (IMS, http://www.natice.noaa.gov/ims/) 24 and 4 km resolution grid products (Helfrich et al., 2007) were also available for comparison. The IMS 4 km product is available since 2004. Ice-on and ice-off dates (binary value: ice vs. open water) at the pixel level as well as CFO dates (all pixels coded as ice) and WCI dates (all pixels coded as open water) on both GBL and GSL were derived for the period 2004–2009. The 4 km IMS product was used for cross-comparison.

TCD
5, 3129–3173, 2011

CIS weekly observations of GBL and GSL ice cover were obtained from 2002–2009. Analysts at the CIS determine a single lake-wide ice fraction value in tenths ranging from 0 (open water) to 10 (complete ice cover) every Friday from the visual interpretation of NOAA AVHRR (1 km pixels) and Radarsat ScanSAR images (100 m pixels) compiled over a full week for many lakes across Canada, including GBL and GSL. CFO and WCI dates can be derived from this product with about a one-week accuracy. CFO was determined as the date when the ice fraction changes from 9 to 10 and remains at this value for the winter period, while WCI was determined as the date when the lake-ice fraction passes from 1 to 0. Lake-wide CFO and WCI dates were derived for all ice seasons corresponding to the AMSR-E (2002–2009) observations.

Finally, MODIS quick look images of GBL and GSL (2002–2009) were downloaded from the Geographic Information Network of Alaska (GINA) (http://www.gina.alaska.edu) for general visual comparison with AMSR-E derived ice products during spring break-up. No suitable images were available during fall freeze-up due to long periods of extensive cloud cover and polar darkness. The MODIS quick-look images are provided as true-color composites (Bands 1, 4, 3 in RGB) – Band 1 (250-m, 620–670 nm), Band 4 (500-m, 545–565 nm), and Band 3 (500-m, 459–479 nm).

5 Ice phenology algorithm

5.1 Examination of T_B evolution during ice-cover and ice-free seasons

The development of a new algorithm for determining various ice phenological parameters through ice seasons required first to examine the seasonal evolution of horizontally and vertically polarized T_B at different frequencies. The sensitivity of T_B at 18.7, 23.8, 36.5, and 89 GHz to ice phenology was examined by selecting one pixel located in the central section of GBL (66° N, 120°30′ W) and two in the main basin of GSL (61°19.8′ N, 115° W and 61°41.8′ N, 113°49.5′ W) (see Fig. 1). Air temperature data from nearby meteorological stations were used in support of the analysis of the temporal evolution of the AMSR-E T_B to detect ice phenological events during the freeze-up and break-up periods at the three sampling sites (pixels) that could then guide the development of the ice phenology algorithm. Although the temporal evolution was examined at the three sites and for all years (2002–2009), for sake of brevity, one site on GBL from 2003–2004 is used to illustrate the general sensitivity of T_B during the freeze-up and break-up periods (Fig. 2). The bottom panel of Fig. 2 shows the time series of maximum/mean air temperatures and snow depth from the Deline meteorological station, while the top and middle panels display the evolution of T_B at four different frequencies and two polarizations (H-pol and V-pol) for the same time period. Changes in T_B are interpreted separately below for the freeze-up and the break-up periods.

5.1.1 Freeze-up period

Using the sampling site on GBL as an example (see Fig. 1), when surface air temperature falls below the freezing point (Fig. 2), the expected increase in T_B with the onset of ice cover formation lags due to the large heat capacity causing delayed ice formation of GBL. This is also observed over GSL (not shown). As shown in Fig. 2, it takes about four to six weeks for the central part of GBL to show the beginning of the freeze-up process. T_B then starts to increase rapidly in association with an increase in fractional ice coverage (FO to ice-on). The significant increase in T_B continues until latent and sensible heat fluxes reach zero across the lake surface around the ice-on date. The distinct increase of T_B is more strongly apparent at horizontal polarization (Fig. 2, upper) for which T_B increases by approximately 70–80 K from open water (ice-free season) to ice-on conditions, compared to vertical polarization (Fig. 2, middle) for each frequency.

From the ice-on date near mid-December to the onset of melt (MO), the increase in T_B is due to ice growth and thickening until lake ice reaches its maximum thickness around mid-April. An increase in T_B is expected during the ice growth season since thicker ice reduces the influence of the lower emissivity (radiometrically cold) liquid water below the ice (Kang et al., 2010). The slope (rate of change) of T_B with time is steeper at 18.7 GHz than at 23.8, 36.5 and 89 GHz during ice growth due to greater penetration depth at lower frequencies. The rate of increase in T_B with ice thickening slows down more quickly at the higher frequencies as the ice becomes thicker (Duguay et al., 2003). The oscillating behavior of T_B at H-pol and V-pol during the ice growth period depends greatly on the imaginary part of the index of refraction of ice (Chang et al., 1997; Kang et al., 2010). Differences in T_B among different frequencies are negligible once the lake ice/snow on ice surface becomes wet during warm winter episodes and starting with MO.

5.1.2 Break-up period

Once the mean air temperature begins to surpass 0 °C, T_B increases rapidly as a result of the higher air temperature and increasing shortwave radiation absorption (decreasing albedo) at the ice/snow surface. The wetter the snow cover becomes, the more the observed T_B also increases due to snow's high emissivity during the break-up period (Jeffries et al., 2005b). The internal structure of the ice becomes uniform, but its surface roughness increases during the melting process (Kouraev et al., 2007b). Albedo on the upper surface of the lake ice continues to decrease from MO until ice-off date because of the removal of snow cover and wind-roughened melt ponds (Howell et al., 2009; Williams and Stefan, 2006). From MO to ice-off dates, the latent heat flux gradually increases, but the sensible heat flux increases negatively (Rouse et al., 2008b). As the open-water area increases, water vaporization and sensible heat flux increase on both GBL and GSL. From the end of May until early June, the ice break-up on GSL leads to rapid bulk heat exchange on the lake surface (Blanken et al., 2007).

As shown in Fig. 2, during the break-up period on GBL, melt-refreeze events lead to fluctuations in T_B at 18.7–89 GHz along the general spring melt trajectory starting with MO. A similar pattern is noticeable from T_B values analyzed over GSL (not shown). Compared with clear ice or black ice, snow ice during break-up absorbs less incident radiation due to its higher albedo, and break-up is delayed as a result of the higher albedo (Jeffries et al., 2005a). However, clear ice, which is typically found on GBL and GSL, allows greater penetration of solar radiation to create internal melt (Woo et al., 2007). The existence of clear ice causes a rapid break-up process, resulting in decreasing T_B. First snow, then snow ice (if any), and finally black ice melt sequentially; the H-pol and V-pol T_B drop rapidly until the ice-off date (Fig. 2). During the middle of July, T_B, which is affected by the radiometrically cold (low emissivity) freshwater, significantly decreases by about 100–140 K from ice-covered to ice-free (open water) conditions.

5.2 Justification of choice of frequency and polarization for algorithm

Based on the overall examination of the evolution of T_B during the ice and ice-free seasons on GBL and GSL at different frequencies and polarizations, 18.7 GHz H-pol measurements appear to be the most suitable for the development of an ice phenology algorithm. Although H-pol is more sensitive than V-pol to wind-induced open water surface roughness, it also shows a larger rise in T_B from open water to ice cover during the later freeze-up and earlier break-up periods. Thus, it is easier to determine T_B thresholds (described in the section below) related to ice phenological parameters at H-pol than at V-pol during those periods. Second, 89 GHz is known to be more sensitive to atmospheric contamination (Kelly, 2009) and is also strongly affected by open water surface roughness from wind, particularly at H-pol. This later effect is also apparent at 23.8 and 36.5 GHz. Occasionally high T_B values at 23.8 and 36.5 GHz during the open water season make it difficult to detect the timing of FO and ice-off dates. Overall, 18.7 GHz H-pol shows less limitations for detecting a broader range of ice phenological parameters (FO, ice-on, MO, and ice-off) than the other channels.

5.3 Determining thresholds for retrieval of ice phenological parameters

A flowchart showing the processing steps for determining the ice phenological parameters is given in Fig. 3. Based on the analysis of T_B values at the three test sites on GBL/GSL over seven ice seasons, a suite of criteria (minimum and maximum

TCD
5, 3129–3173, 2011

thresholds, averages of preceding and succeeding days, and threshold value of number of days to the maximum T_B in the time series, DistM) was devised to detect FO, ice-on, MO, and ice-off dates.

5.3.1 Freeze-up period

The FO date is detected during the upturn of T_B from an open water surface. A maximum T_B threshold value of 180 K is high enough to avoid confusion with fluctuating T_B values influenced by wind-induced roughness of the open water surface. Then, in order to discriminate T_B under open water conditions from the starting point of FO, the average taken from the succeeding twenty days for each individual day of the time series is calculated. This average value must fall within the range of 110 K and 140 K. The last criterion consists of finding the maximum T_B value in the time series, which is reached late during the ice season. Once found, the number of days from each day to that of the maximum T_B (DistM in Fig. 3) is calculated. DistM must be less than 250 days, in addition to falling within the threshold T_B values given above, for the algorithm to be able to detect FO. For detecting the ice-on date, first maximum and minimum threshold values of 195 K and 160 K are used. Then, as an extra criterion to distinguish between the FO date and ice-on date, the average T_B value of the 15 days preceding each individual day in the time series has to fall between 100 and 155 K. Lastly, DistM must be less than 220 days.

5.3.2 Break-up period

For the determination of the MO date, maximum and minimum threshold values are set to 240 K and 160 K. Then, for discriminating the starting point of MO from other days during the ice growth/thickening season, the average T_B calculated from the previous fifteen days of each individual day in the time series must fall between 165 K and 225 K threshold and with a DistM of less than 70 days. The ice-off date is detected from a sharp drop in T_B from that of the melt period that starts with MO (Fig. 2). For this last phenological parameter, the maximum and minimum thresholds are set to 140 K and 210 K. To ensure discrimination of this first day of the ice-free season to those of later days, the average T_B value of the preceding five days is fixed to 160 K and with DistM less than 60 days.

6 Results and Discussion

6.1 Spatio-temporal variability of lake ice phenological parameters

The algorithm described above was applied to all interpolated 10 km pixels on GBL and GSL for every day during the period 2002–2009 to produce maps of FO, ice-on, MO and ice-off dates, as well as freeze duration (FD), melt duration (MD), and ice cover duration (ICD) averaged over all years (Figs. 4, 5). Recognizing that the relatively coarse spatial resolution of the product leads to a certain level of land contamination in T_B values along lakeshores and where a high concentration of islands exists (e.g. eastern arm of GSL), confidence regions were drawn on the two lakes with an outer buffer zone of 10 km. Average dates and duration of the ice phenological parameters calculated from all pixels over the greatest extent as possible for the lakes as well as within the confidence regions are included in Tables 3–5. Interestingly, in Tables 3–5 one can see that the standard deviations of ice phenological parameters are almost always larger for GSL than for GBL, indicating that ice phenological processes are generally more variable spatially (i.e. between pixels) on the former lake which is located at a more southern latitude.

6.1.1 Freeze-up period

Once water cools to the freezing point, ice begins to form first in shallow near shore areas. Freeze-up is influenced primarily by air temperature and to a lesser extent by wind, in addition to lake depth. On average, the date of FO occurs approximately one week earlier on GBL than on its southern counterpart, GSL (Table 3). For GBL, the latest FO date over the study period occurred during ice season 2008–2009 (Day of Year or DY 330, late November) followed by 2003–2004 (DY 322). The earliest FO date happened in 2004–2005 (DY 308, early November), closely followed by 2005–2006 (DY 314). For GSL, both the 2005–2006 and 2008–2009 ice seasons experienced the latest FO dates of DY 332 and 342, respectively. The earliest FO date occurred in 2006–2007 on DY 316, closely followed by 2004–2005 (DY 322). In addition to the effect of fall temperature in explaining earlier/later FO dates, an early ice break-up (longer period of solar radiation absorption by water) and warmer summer of the preceding months can result in the late onset of freeze-up for the two large, deep, lakes that store a considerable amount of heat during the open water season (Brown and Duguay, 2010). The latter process may be the case for ice season 2008–2009. Noteworthy is the fact that, in contrast to GBL, GSL's timing of ice formation is somewhat influenced by river inflow from the Slave River in its southeast section (Howell et al., 2009). A slight delay in FO is noticeable during most years at its mouth (see Figs. 1 and 4). GBL's ice regime is not affected by such inflow (Fig. 4).

Similar to FO, ice-on occurs approximately one week later on GSL than on GBL. The average ice-on date occurs on DY 333 and 343 for GBL and GSL, respectively (Table 3). Schertzer et al. (2008) and Walker et al. (2000) estimated average CFO in the main basin of the GSL to occur on DY 342 for the period 1988–2003. Spatially, for GBL (Fig. 4 and Table 3), the ice-on dates take place in the Central Basin around early December, except for 2004–2005 (end November). For GSL, the ice-on dates occur in mid-December with the exception of 2008–2009 (end December). Similar to FO, both lake depth (heat storage) and air temperature are the two main variables explaining the spatio-temporal variability of ice-on dates on the two lakes.

The freeze duration (FD), which encompasses the period from FO to ice-on, takes two to three weeks on both lakes. For GBL, the longest FD over the study period happened during ice season 2003–2004 (28 days), closely followed by 2005–2006 and 2007–2008 (26 days). The shortest FD occurred in 2008–2009 (10 days) (Table 3). For GSL, the longest FD took place during ice season 2005–2006 (27 days), followed by

TCD
5, 3129–3173, 2011

Estimating ice phenology on large northern lakes from AMSR-E

K.-K. Kang et al.

2006–2007 (19 days) while the shortest FD happened in 2008–2009 (9 days) (Table 3). FD in GBL usually takes about 1–2 weeks longer than that in GSL, likely due to the fact that depths within the confidence region of GBL range from 50 and 200 m, while they vary between 20 and 80 m in GSL, therefore GBL taking a longer time to lose its heat. One exception is ice season 2005–2006 for which FD is 1–2 days longer in GSL. Warmer average fall temperature in 2005 and earlier ice-off date in the preceding season (i.e. DY 155 in 2005), the latter having an impact on the open water duration (and amount of stored heat), are the likely reasons for the relatively longer FD in GSL for ice season 2005–2006 compared to other ice seasons.

Freezing Degree Days (FDD), calculated as the sum of mean daily air temperatures below 0 °C measured at a meteorological station, and given in the bottom left of Fig. 4, provide some indication of the effect of colder/warmer temperatures on FD (FDD calculated here between FO to ice-on date) in each ice season. It must be bear in mind, however, that heat storage during the preceding open water season will also have an impact on FD. Due to this, the relation between FDD and FD is therefore not always consistent from year to year for the two lakes.

6.1.2 Break-up period

The break-up process is primarily influenced by air temperature variability, causing earlier or later MO dates on the two lakes. The MO dates mark the beginning of melt of snow on the ice surface or the initiation of melt of ice in the case when a bare ice surface is encountered. Differences in the timing of MO between GBL and GSL can largely be explained by contrasting spring air temperatures due to their latitudinal position. MO dates occur approximately one week earlier on GSL than on GBL (Table 4). The average MO date occurs on DY 143 (end May) on GBL and DY 135 (mid May) on GBL (see Fig. 5). For GBL, the earliest MO dates happened on DY 127 (2002–2003), closely followed by DY 128 (early May) in 2005–2006. The latest MO dates for this lake happened in 2003–2004 (DY 155, early June) and in 2008–2009 (DY 168, mid June) (Table 4). For GSL, the earliest MO date occurred on DY 122 (early May) in 2005–2006

TCD
5, 3129–3173, 2011

and the latest date took place in 2003–2004 (DY 150, early June), followed by 2002–2003 and 2008–2009 (DY 137). The warmer average spring air temperature (−7.8 °C and −1.0 °C for GBL and GSL, respectively) caused earlier MO dates to occur in ice season 2005–2006, while the colder spring of ice season 2003–2004 (−11.7 °C and −7.6 °C for GBL and GSL, respectively) resulted in later MO dates.

In contrast to MO, the average ice-off dates on GSL are about four weeks earlier (DY 157, early June) than on GBL (DY 183, early July) (see Fig. 5). For GBL, the latest ice-off date occurred during ice season 2003–2004 on DY 198 (mid July), closely followed by 2008–2009 on DY 197. The earliest ice-off date occurred in 2005–2006 on DY 169 (mid June) (Table 4). For GSL, both ice seasons 2003–2004 and 2008–2009 experienced the latest ice-off dates of DY 169 and 167 (mid June), respectively. The earliest ice-off date for this lake happened in 2005–2006 on DY 140 (mid May) (Table 4). Early ice-off dates lengthen the open water season during the high solar period in spring/summer, resulting in a longer period of solar radiation absorption by the lakes and, subsequently, higher lake temperatures in late summer/early fall due to larger heat storage. Looking at specific ice cover seasons, the colder spring/early summer climate conditions of 2004 and 2009 contributed to later break-up, while the warmest conditions of 2006 influenced earlier break-up (Table 4). On GSL, ice-off dates are earlier in the majority of years at the mouth of the Slave River which brings warmer water as this river flows from the south into the lake (see Fig. 5). For GBL, however, ice-off dates are not influenced by similar river inflow such that spatially melt generally proceeds gradually from the more southern (warmer) to the northern sections of the lake. Unlike MO, the larger difference in ice-off dates between the two lakes (about four weeks) can be explained by a combination of thicker ice and colder spring/early summer conditions at GBL which, as a result, requires a greater number of days above 0 °C to completely melt the ice.

The average melt duration (MD), which encompasses the period from MO to ice-off, takes two to five weeks longer on GBL than on GSL with the exception of ice season 2008–2009 which had comparable MD (Table 4). For GBL, the longest MD lasted

TCD
5, 3129–3173, 2011

Estimating ice phenology on large northern lakes from AMSR-E

K.-K. Kang et al.

54–55 days in 2002–2003/2004–2005, followed by 43–46 days in 2003–2004/2006–2007. The shortest MD was rapid at 28 days in 2008–2009 (Table 4). For GSL, the longest MD lasted 30 days in 2008–2009, followed by 20 days in 2004–2005/2006–2007, whereas the shortest MD took 17 days in 2005–2006 (Table 4). The length of the MD is mainly controlled by the combination of end-of-winter maximum ice thicknesses and spring/early summer temperatures. In general, the thinner the ice is before melt begins and the warmer the temperature conditions are between MO and ice-off, the shorter the MD lasts. One exception is the central basin of GSL, where MD is also influenced by the inflow of water from Slave River which helps to accelerate the break-up process in this lake. Melting Degree Days (MDD), calculated as the sum of mean daily air temperatures above 0 °C at a meteorological station from MO until ice-off, provide some indication of the effect of colder/warmer temperatures in spring/early summer on MD for each ice season (see bottom left corner of Fig. 5). Visually, a relation appears to exist between long/short MD and low/high MDD for GBL. Such a relation does not seem to be present for GSL, likely as a result of the inflow of water from Slave River which helps to melt the ice both vertically at ice underside and laterally at the ice edge.

6.1.3 Ice cover duration

The average ice cover duration (ICD), which is calculated as the number of days between ice-on and ice-off dates, is one week shorter for GSL than for GBL over the full period of analysis (DY 218 and 211 on average, respectively). However, the length of the ICD can differ by as much as four to five weeks between the two lakes in some years. For GBL, the longest ICD was 229 days in 2004–2005, followed by 226 days in 2003–2004, while the shortest lasted 203 days (2005–2006). For GSL, the longest ICD lasted 223 days (2003–2004), closely followed by 220 days in 2002–2003, while the shortest was 193 days (2007–2008) (Table 5). In GBL's Smith Arm and Dease Arm (northern section of lake), lake ice stays longer than in the other arms, up until the middle (or end) of July (Fig. 5), particularly during the two cold winter seasons of

2003–2004 and 2008–2009. For GSL, shorter ICD occurs at the mouth of Slave River and near Yellowknife compared to the east arm of the lake (Fig. 5). ICD is influenced by river inflow from Slave River for the full period of study (2002–2009), as it has a particularly large influence on ice-off dates (see Fig. 5).

6.2 Comparison of AMSR-E ice phenological parameters with other satellite-derived ice products

While the AMSR-E retrieval algorithm captures well the spatial patterns and seasonal evolution of ice cover on GBL and GSL over several ice seasons, estimated dates of the various ice phenological parameters should be cross-compared to those determined from other approaches (methods and satellite sensors) whenever possible as to provide at least a qualitative assessment of the level of agreement between existing products. A detailed quantification of uncertainty (biases) of the various ice products is, however, beyond the scope of this paper. This is a topic that merits to be investigated in a follow-up study encompassing a larger number of lakes.

6.2.1 Comparison with other pixel-based products

Tables 6–8 present summary statistics of ice phenological parameters estimated at the pixel level from AMSR-E T_B (2002–2009) against those obtained with daily QuikSCAT (2002–2006; Howell et al., 2009) and NOAA/IMS products (2004–2009). Values in these tables are the averages and standard deviations calculated from all pixels over the complete lakes and their main basin (confidence regions). IMS ice parameters consist of ice-on/ice-off dates and ICDp, while QuikSCAT-derived parameters are comprised of FO/MO/ice-off dates and ICDp calculated from FO to ice-off dates. The complex nature of the freeze-up process has been reported to make the distinction between FO and ice-on dates difficult from analysis of the temporal evolution of backscatter ($\sigma°$) from QuikSCAT (Howell et al., 2009). This can be explained by the fact that QuikSCAT-derived ice phenological parameters are influenced by deformation features such as ice

TCD
5, 3129–3173, 2011

rafts, wind-roughened cracks, and ridge formation during the freeze-up period, acting to increase σ°. However, time series of AMSR-E T_B at 18.7 GHz (H-pol) can differentiate FO from ice-on dates (see Fig. 2) as T_B is largely controlled by changes in emissivity progressively from the radiometrically cold open water to the warmer ice-covered lake surface, not as much by lake ice surface roughness, during the freeze-up period.

FO dates as determined from AMSR-E are about one week earlier on average (7–11 days for GBL; 1–8 days for GSL) than those derived with QuikSCAT when considering the two lakes over the five years available for comparison (Table 6). AMSR-E T_B may be more sensitive to within-pixel fractional presence of ice and less to wind-induced surface roughness over open water areas than σ° from QuikSCAT. Regarding ice-on dates, AMSR-E (from DY 323 to 352) and IMS (from DY 319 to 338) show a difference of about one week on average, with AMSR-E detecting ice-on later. In fact, and as illustrated in Figs. 6–7, NOAA/IMS ice-on patterns follow AMSR-E FO more closely than ice-on. Interestingly, IMS ice-on remains the same between DY 324 and DY 335 on GSL (Fig. 7) while FO evolves over the same period in AMSR-E. This indicates that the presence of extensive cloud cover over this period may have been a limiting factor in determining the presence of ice and open water on GSL by ice analysts who largely rely on the use of optical satellite data in preparing the IMS product.

The difference in MO dates is very variable between AMSR-E and QuikSCAT, ranging anywhere between a single day to four weeks (Table 7). During the break-up period, σ° seems more sensitive to initial surface melt than T_B with QuikSCAT providing in all but one case earlier MO. AMSR-E (from DY 140 to 198) and QuikSCAT ice-off dates (from DY 151 to 205) show similar inter-annual variability with a difference of about one week (Table 7). Average ice-off dates are also quite close between AMSR-E and IMS with a difference of approximately five days. They also follow the same variability (later and earlier dates) between years. Although the number of years in this cross-comparison between products is somewhat limited, these initial results suggest that ice-on is the most consistent ice phenological parameter across products examined herein. This point is further supported by the similar spatial patterns in ice-on/ice-off

TCD
5, 3129–3173, 2011

determined from AMSR-E, IMS, and MODIS imagery over the break-up period of ice season 2005–2006 (Figs. 8 and 9).

AMSR-E ICDp differs by one week on average with IMS (Table 8). Ice cover is estimated to remain longer with IMS when examining the full extent of GBL and GSL. This is expected since IMS is a finer resolution product (4 km) that can resolve ice in areas of the lakes where AMSR-E has a harder time due to land contamination (along lake shore and areas with small islands as in the east arm of GSL). When considering only the main basin sections of GBL and GSL (confidence regions), AMSR-E ICDp estimates are slightly shorter for GBL and longer for GSL. Since ICDp is calculated from ice-on to ice-off dates such differences are possible. As indicated earlier, ice-on dates from IMS tend to fall between FO and ice-on dates from AMSR-E, but closer to FO. Differences in ICDp tend to be larger between AMSR-E and QuikSCAT estimates over two lakes, the main reason being that ICDp from QuikSCAT was calculated from FO, instead of ice-on to ice-off dates by Howell et al. (2009). This makes the comparison a bit more tentative than with the IMS product.

6.2.2 Lake-wide comparison

Table 9 shows summary statistics of CFO, WCI and ICDe estimated with AMSR-E against those determined from NOAA/IMS and by CIS. CFO corresponds to the date when all pixels within a lake or lake section become totally ice-covered (i.e. 100 % ice fraction), while WCI is the date when all pixels become ice-free (i.e. 100 % open water). ICDe is calculated as the number of days between CFO and WCI. In Table 9, CFO/WCI/ICDe estimates from IMS and CIS are for the entire extent of GBL and GSL. Acknowledging that estimates of the same parameters are derived at a coarser spatial resolution with AMSR-E, estimates are provided for both the entire lake surfaces and main basins only (confidence regions) of GBL and GSL. Also noteworthy is the fact that CIS is weekly product, unlike the IMS and AMSR-E products that are derived daily. Therefore, some of the differences between estimated dates may be attributed to the temporal resolution of the products. AMSR-E/CFO (from DY 330 to 356)

TCD
5, 3129–3173, 2011

dates compare well with CIS/CFO (from DY 324 to 354) and IMS/CFO (from DY 326 to 348), as do AMSR-E/WCI (from DY 158 to 210) with IMS/WCI (from DY 175 to 209) and CIS/WCI (from DY 165 to 219). Overall, these results are very encouraging since CFO/WCI/ICDe estimated with the new automated AMSR-E ice phenology retrieval algorithm are within about one week of those determined by ice analysts (IMS and CIS) through visual interpretation of imagery from various sources (optical and SAR). Some of the variability in estimates between years (earlier/later dates) should, however, be examined more closely in a follow-up study.

7 Conclusions

The 18.7 GHz (H-pol) was found to be the most suitable AMSR-E channel for estimating ice phenological dates. It is less sensitive than the other frequencies examined to wind effects over open water and H-pol is better than V-pol for discriminating open water from ice. As a result, an ice phenological retrieval algorithm which makes use of AMSR-E 18.7 GHz H-pol T_B data was developed and applied to map the evolution of freeze-onset/melt-onset and ice-on/ice-off dates, as well as melt/freeze/ice cover duration on GBL and GSL over seven ice seasons (2002–2009). Through this, much was learned about the temporal and spatial evolution of ice cover within and between the two large lakes in relation to regional climate, latitudinal position, lake depth and, in the case of GSL, the influence of water inflow from Slave River. Results revealed that during the freeze-up period both freeze-onset and ice-on dates occur about one week earlier, and freeze duration lasts approximately one week longer on GBL than on GSL. During the break-up period, melt-onset and ice-off dates happen on average one week and approximately four weeks later, respectively, on GBL. Located in a colder climate region, melt duration lasts about three weeks longer on this lake compared to its southern counterpart. The net effect is that ice cover duration is usually three to four weeks longer, depending on the ice season, on GBL compared to GSL. These results add to our knowledge of ice phenology on the two lakes which had not been fully documented and contrasted in previous investigations.

TCD
5, 3129–3173, 2011

Results from an initial cross-comparison between AMSR-E estimated ice phenological parameters and those estimated by QuikSCAT, as well as those obtained from NOAA IMS and CIS show that relatively coarse resolution AMSR-E 18.7 GHz H-pol T_B data are suitable for monitoring of ice phenology on the two lakes, at least in their main basins in a consistent manner. The ice phenology algorithm described in this paper may be applicable to other large lakes of the Northern Hemisphere and also to longer time series of passive microwave satellite data from SMMR-SSM/I (circa 32-yr historical record). These are two lines of research that we are actively pursuing.

Acknowledgements. This research was supported by a NSERC Discovery Grant to C. Duguay. The AMSR-E/Aqua level 2A (AE_L2A) and IMS daily Northern Hemisphere snow and ice analysis data products were obtained from the National Snow and Ice Data Center Distributed Active Archive Center (NSIDC DAAC), University of Colorado at Boulder. Weekly ice cover fraction data was provided by the Canadian Ice Service (CIS).

References

Barry, R. G. and Maslanik, J. A.: Monitoring lake freeze-up/break-up as a climatic index. In Snow Watch '92. Detection strategies for snow and ice, World Data Center for Glaciology Report GD-25, edited by: Barry, R. G., Goodison, B. E., and LeDrew, E. F., NSIDC: Boulder CO, 66–77, 1993.

Blanken, P., Rouse, W., and Schertzer, W. M.: Time scales of evaporation from Great Slave Lake: Cold Region Atmospheric and Hydrologic Studies: The Mackenzie GEWEX Experience Volume 2: Hydrologic Processes, edited by: Woo, M.-K., Springer, 181–196, 2007.

Bonsal, B. R., Prowse, T. D., Duguay, C. R., and Lacroix, M. P.: Impacts of large-scale teleconnections on freshwater-ice duration over Canada, J. Hydrol., 330, 340–353, 2006.

Brown, L. C. and Duguay, C. R.: The response and role of ice cover in lake-climate interactions, Prog. Phys. Geog., 34, 671–704, doi:10.1177/0309133310375653, 2010.

Chang, A. T. C., Foster, J. L., Hall, D. K., Goodison, B. E., Walker, A. E., Metcalfe, J. R., and Harby, A.: Snow parameters derived from microwave measurements during the BOREAS winter field campaign, J. Geophys. Res., 102, 29663–29671, 1997.

Duguay, C. R., Flato, G. M., Jeffries, M. O., Ménard, P., Morris, K., and Rouse, W. R.: Ice-cover variability on shallow lakes at high latitudes: model simulations and observations, Hydrol. Process., 17, 3465–3483, 2003.
Duguay, C. R., Prowse, T. D., Bonsal, B. R., Brown, R. D., Lacroix, M. P., and Ménard, P.: Recent trends in Canadian lake ice cover, Hydrol. Process., 20, 781–801, 2006.
Helfrich, S. R., McNamara, D., Ramsay, B. H., Baldwin, T., and Kasheta, T.: Enhancements to, and forthcoming developments in the Interactive Multisensor Snow and Ice Mapping System (IMS), Hydrol. Process., 21, 1576–1586, 2007.
Hewison, T. J.: Airborne measurements of forest and agricultural land surface emissivity at millimeter wavelengths, IEEE T. Geosci. Remote, 39, 393–400, 2001.
Hewison, T. J. and English, S. J.: Airborne retrievals of snow and ice surface emissivity at millimeter wavelengths, IEEE T. Geosci. Remote, 37, 1871–1879, 1999.
Howell, S. E. L., Brown, L. C., Kang, K. K., and Duguay C. R.: Variability in ice phenology on Great Bear Lake and Great Slave Lake, Northwest Territories, Canada, from SeaWinds/QuikSCAT: 2000–2006, Remote Sens. Environ., 113, 816–834, 2009.
Jeffries, M. O. and Morris, K.: Some aspects of ice phenology on ponds in central Alaska, USA, Ann. Glaciol., 46, 397–403, 2007.
Jeffries, M. O., Morris, K., and Duguay, C. R.: Lake ice growth and decay in central Alaska, USA: observations and computer simulations compared, Ann. Glaciol., 40, 195–199, 2005a.
Jeffries, M. O., Morris, K., and Kozlenko, N.: Ice characteristics and processes, and remote sensing of frozen rivers and lakes in remote sensing in northern hydrology: Measuring environmental change, edited by: Duguay, C. R. and Pietroniro, A., Geophysical Monograph, 163, American Geophysical Union, 63–90, 2005b.
Kang, K.-K., Duguay, C. R. Howell, S. E. L., Derksen, C. P., and Kelly, R. J.: Seasonal evolution of lake ice thickness in Great Bear and Great Slave Lakes from AMSR-E, IEEE Geosci. Remote Sens. Lett., 7, 751–755, 2010.
Kelly, R. E. J.: The AMSR-E snow depth algorithm: Description and initial results, J. Remote Sens. Soc. Japan, 29, 307–317, 2009.
IGOS: Integrated Global Observing Strategy Cryosphere Theme Report, WMO/TD-No. 1405, World Meteorological Organization, Geneva, 100 pp., 2007.
Kouraev, A. V., Semovski, S. V., Shimaraev, M. N., Mognard, N. M., Légresy, B., and Remy, F.: Observations of Lake Baikal ice from satellite altimetry and radiometry, Remote Sens. Environ., 108, 240–253, doi:10.1016/j.rse.2006.11.010, 2007a.

Kouraev, A. V., Semovski, S. V., Shimaraev, M. N., Mognard, N. M., Légresy, B., and Remy, F.: The ice regime of Lake Baikal from historical and satellite data: Relationship to air temperature, dynamical, and other factors, Limnol. Oceanogr., 52, 1268–1286, 2007b.

Latifovic, R. and Pouliot, D.: Analysis of climate change impacts on lake ice phenology in Canada using the historical satellite data record, Remote Sens. Environ., 106, 492–508, 2007.

Magnuson, J. J., Robertson, D. M., Benson, B. J., Wynne, R. H., Livingstone, D. M., Arai, T., Assel, R. A., Barry, R. G., Card, V., Kuusisto, E., Granin, N. G., Prowse, T. D., Stewart, K. M., and Vuglinski, V. S.: Historical trends in lake and river ice cover in the northern hemisphere, Science, 289, 1743–1746, doi:10.1126/science.289.5485.1743, 2000.

Maslanik, J. A. and Barry, R. G.: Lake Ice Formation and Breakup as an Indicator of Climate Change: Potential for Monitoring Using Remote Sensing Techniques. The Influence of Climate Change and Climatic Variability on the Hydrologic Regime and Water Resources, International Association of Hydrological Sciences Press, IAHS Publ. No. 168, 153–161, 1987.

Rouse, W. R., Binyamin, J., Blanken, P. D., Bussières, N., Duguay, C. R., Oswald, C. J., Schertzer, W. M., and Spence, C.: The Influence of Lakes on the Regional Energy and Water Balance of the Central Mackenzie River Basin. Cold Region Atmospheric and Hydrologic Studies: The Mackenzie GEWEX Experience Volume 1: Atmospheric Processes, edited by: Woo, M.-K., Springer, 309–325, 2008a.

Rouse, W. R., Blanken, P. D., Bussières, N., Oswald, C. J., Schertzer, W. M., Spence, C., and Walker, A. E.: An Investigation of the Thermal and Energy Balance Regimes of Great Slave and Great Bear Lakes, J. Hydrom., 9, 1318–1333, 2008b.

Schertzer, W. M, Rouse, W. R., Blanken, P. D., Walker, A. E., Lam, D. C. L., and León, L.: Interannual Variability of the Thermal Components and Bulk Heat Exchange of Great Slave Lake, Cold Region Atmospheric and Hydrologic Studies: The Mackenzie GEWEX Experience Volume 2: Hydrol. Process., edited by: Woo, M.-K., Springer, 197–219, 2008.

Ulaby, F. T., Moore, R. E., and Fung, A. K.: Microwave remote sensing: active and passive, Vols. 1, 2 and 3, Addison-Wesley Publishing Company, MA, 1986.

Walker, A. E. and Davey, M. R.: Observation of Great Slave Lake ice freeze-up and break-up processes using passive microwave satellite data, Proceedings of 16th Symposium on Remote Sensing, Sherbrooke, QC, Canada, L'AQT/CRSS, 233–238, 1993.

Walker, A. E., Silis, A, Metcalf, J. R., Davey, M. R., Brown, R. D., and Goodison, B. E.: Snow

cover and lake ice determination in the MAGS region using passive microwave satellite and conventional data, Proc. 5th Scientific Workshop, Mackenzie GEWEX Study, Edmonton, Alberta, Canada, 39–42, 2000.
Williams, S. G. and Stefan, H. G.: Modeling of lake ice characteristics in north America using climate, geography, and lake bathymetry, J. Cold Regions Eng., 20, 140–167, 2006.
Woo, M.-K., Modeste, P., Martz, L., Blondin, J., Kochtubajda, B., Tutcho, D., Gyakum, J., Takazo, A., Spence, C., Tutcho, J., Di Cenzo, P., Kenny, G., Stone, J., Neyelle, I., Baptiste, G., Modeste, M., Kenny, B., and Modeste, W.: Science meets traditional knowledge: water and climate in the Sahtu (Great Bear Lake) region, Northwest Territories, Canada, Arctic, 60, 37–46, 2007.
Woo, M.-K., Rouse, W. R., Stewart, R. E., and Stone, J. M. R.: The Mackenzie GEWEX Study: A contribution of cold region atmospheric and hydrologic sciences, Cold Region Atmospheric and Hydrologic Studies: The Mackenzie GEWEX Experience Volume 1: Atmospheric Processes, edited by: Woo, M.-K., Springer, 181–196, 2008.

TCD
5, 3129–3173, 2011

Estimating ice phenology on large northern lakes from AMSR-E

K.-K. Kang et al.

Table 1. Definition of ice phenological parameters at per pixel level and for entire lake or lake section.

	Pixel level	Entire lake or lake section
Freeze-up Period	**Freeze onset (FO)**: first day of the year on which the presence of ice is detected in a pixel and remains until ice-on **Ice-on**: day of the year on which a pixel becomes totally ice-covered **Freeze duration (FD)**: number of days between freeze-onset and ice-on date	**Complete freeze over (CFO)**: day of the year when all pixels become totally ice-covered
Break-up period	**Melt onset (MO)**: first day of the year on which generalized spring melt begins in a pixel **Ice-off**: day of the year on which a pixel becomes totally ice-free **Melt duration (MD)**: numbers of days between melt-onset and ice-off dates	**Water clear of ice (WCI)**: day of the year when all pixels become totally ice-free
Ice season	**Ice cover duration (ICDp)**: number of days between ice-on and ice-off dates	**Ice cover duration (ICDe)**: number of days between CFO and WCI

TCD
5, 3129–3173, 2011

Table 2. Seasonal mean air temperature (˚C) for winter (DJF), spring (MAM), summer (JJA) and autumn (SON), and annual snowfall (cm) recorded at Deline (GBL), Yellowknife and Hay River combined (GSL) meteorological stations (2002–2009). M indicates missing data. S.D. is standard deviation.

	DJF		MAM		JJA		SON		Annual temp		Annual snowfall (cm)	
	GBL	GSL	GBL	GSL	GBL	GSL	GBL	GSL	GBL	GSL	GBL	GSL
2002	−23.9	−21.5	−10.6	−9.5	11.1	14.2	−3.1	−1.3	−6.0	−4.0	14.6	15.5
2003	−22.1	−20.6	−8.2	−4.3	11.6	14.7	−3.8	−0.3	−6.1	−2.9	22.2	16.2
2004	−24.4	−21.0	−11.7	−7.6	10.4	13.8	−6.9	−2.9	−8.7	−5.1	16.1	16.9
2005	−24.7	−22.9	−6.0	−3.6	10.0	13.6	−5.4	0.0	−5.6	−2.1	25.7	24.1
2006	−20.6	−15.9	−7.8	−1.0	12.1	15.9	−4.9	−2.0	−5.5	−0.9	28.8	24.0
2007	−22.7	−18.7	−9.7	−4.7	11.2	14.6	−5.3	−1.6	−7.0	−3.3	17.0	19.7
2008	−25.0	−23.5	−8.2	−6.0	10.6	15.4	−4.7	0.0	−7.2	−3.9	16.7	26.9
2009	−25.4	−23.8	−10.4	−7.1	10.7	14.2	−4.5	0.1	−7.1	−3.7	M	22.2
Avg	−23.5	−21.8	−8.6	−4.9	11.4	14.5	−4.6	−1.6	−6.3	−3.4	20.2	20.7
S.D.	1.5	2.9	2.0	2.2	0.8	0.9	1.5	1.7	1.1	1.3	5.5	4.2

TCD
5, 3129–3173, 2011

Estimating ice phenology on large northern lakes from AMSR-E

K.-K. Kang et al.

Table 3. Summary of ice phenological parameters during the freeze-up period (average day of freeze-onset (FO) and ice-on, and number of days of freeze duration (FD)) for GBL and GSL (2002–2009). Values within confidence regions in bold. Standard deviation in parentheses.

Year	FO		Ice-On		FD	
	GBL	GSL	GBL	GSL	GBL	GSL
2002–2003	311/**320** (14/**7**)	318/**331** (18/**4**)	328/**333** (11/**7**)	334/**345** (17/**7**)	32/**28** (11/**5**)	31/**19** (17/**10**)
2003–2004	313/**322** (11/**5**)	319/**329** (14/**5**)	332/**337** (8/**5**)	338/**345** (11/**5**)	31/**28** (7/**5**)	27/**15** (15/**7**)
2004–2005	303/**308** (9/**4**)	313/**322** (13/**3**)	321/**323** (6/**4**)	331/**338** (12/**4**)	26/**22** (9/**3**)	24/**12** (13/**6**)
2005–2006	309/**314** (9/**4**)	320/**332** (15/**4**)	326/**330** (8/**4**)	337/**344** (12/**4**)	28/**26** (11/**7**)	30/**27** (18/**20**)
2006–2007	312/**317** (9/**3**)	310/**316** (9/**5**)	331/**335** (7/**3**)	328/**332** (8/**3**)	26/**24** (5/**2**)	24/**19** (9/**7**)
2007–2008	311/**316** (8/**3**)	318/**326** (10/**4**)	329/**333** (8/**4**)	338/**343** (9/**4**)	27/**26** (4/**2**)	24/**16** (10/**6**)
2008–2009	320/**330** (13/**6**)	330/**342** (15/**6**)	334/**340**(8/**4**)	344/**352** (12/**3**)	12/**10** (4/**3**)	15/**9** (8/**5**)
Average	311/**318** (11/**4**)	318/**328** (11/**3**)	329/**333** (6/**4**)	336/**343** (9/**4**)	26/**23** (9/**3**)	25/**17** (11/**7**)

TCD
5, 3129–3173, 2011

Table 4. Summary of ice phenological parameters during the break-up period (average day of melt-onset (MO) and ice-off, and number of days of melt duration (MD)) for GBL and GSL (2002–2009). Values within confidence regions in bold. Standard deviation in parentheses.

Year	MO		Ice-Off		MD	
	GBL	GSL	GBL	GSL	GBL	GSL
2002-03	133/**127** (14/**12**)	132/**137** (14/**5**)	193/**183** (14/**7**)	172/**157** (19/**2**)	61/**55** (15/**12**)	41/**19** (21/**4**)
2003-04	156/**155** (3/**2**)	147/**150** (16/**6**)	203/**198** (7/**4**)	186/**169** (20/**4**)	47/**43** (7/**4**)	39/**19** (19/**7**)
2004-05	133/**132** (11/**7**)	124/**131** (21/**17**)	193/**186** (11/4)	168/**155** (19/**4**)	60/**54** (13/**9**)	44/**24** (20/**17**)
2005-06	129/**128** (7/**4**)	119/**122** (9/**5**)	182/**169** (16/**5**)	161/**140** (21/**6**)	53/**41** (16/**7**)	42/**17** (22/**7**)
2006-07	142/**141** (10/**6**)	124/**129** (17/**6**)	197/**187** (12/**6**)	166/**153** (19/**5**)	55/**46** (13/**10**)	42/**24** (18/**6**)
2007-08	149/**152** (9/**9**)	133/**135** (16/**10**)	187/**183** (10/**4**)	170/**156** (20/**2**)	38/**31** (13/**8**)	37/**20** (20/**9**)
2008-09	167/**168** (8/**7**)	135/**137** (18/**14**)	200/**197** (6/**3**)	177/**167** (16/**3**)	33/**28** (10/**8**)	42/**30** (16/**12**)
Average	144/**143** (6/**3**)	131/**134** (12/**5**)	194/**186** (9/**3**)	171/**157** (17/**3**)	50/**43** (10/**5**)	41/**22** (17/**4**)

TCD
5, 3129–3173, 2011

Table 5. Summary of ice cover duration (ICDp) and open water season (OWS) (average number of days) for GBL and GSL (2002–2009). Values within confidence regions in bold. Standard deviation in parentheses. Note that OWS was not calculated for 2009 since it requires ice-on date to be known for fall freeze-up period 2009, which was not determined in this study.

Year	ICDp		Year	OWS	
	GBL	GSL		GBL	GSL
2002–2003	224/**215** (19/**11**)	195/**220** (28/**29**)	2003	123/**116**(23/**22**)	151/**172** (28/**5**)
2003–2004	233/**226** (12/**7**)	203/**223** **(**22/**22)**	2004	102/**97**(13/**13**)	130/**154** (28/**6**)
2004–2005	232/**229** (10/**7**)	195/**218** **(**20/**22)**	2005	119/**112**(16/**16**)	155/**176** (27/**6**)
2005–2006	210/**203** (15/**7**)	176/**201** **(**26/**26)**	2006	136/**132**(21/**21**)	156/**177** (26/**7**)
2006–2007	225/**217** (14/**8**)	195/**214** (17/**21**)	2007	117/**113** (17/**16**)	155/**172** (24/**7**)
2007–2008	219/**215** (10/**6**)	184/**193** (12/**14**)	2008	134/**125** (20/**20**)	162/**186** (30/**6**)
2008–2009	230/**223** (11/**5**)	193/**208** (18/**19**)			
Average	225/**218** (9/**6**)	192/**211** (16/**18**)	Average	122/**116** (15/**14**)	152/**173** (32/**5**)

TCD
5, 3129–3173, 2011

Estimating ice phenology on large northern lakes from AMSR-E

K.-K. Kang et al.

Table 6. Comparison of ice phenological parameters for freeze-up period (FO and Ice-On) daily-derived from AMSR-E (AME), QuikSCAT (QUT) and NOAA/IMS (IMS) products for GBL and GSL (2002–2009). Values within confidence regions in bold. Standard deviation in parentheses.

Pixel Level	FO				Ice-On			
	GBL		GSL		GBL		GSL	
YEAR	AME	QUT	AME	QUT	AME	IMS	AME	IMS
0203	311/**320** (14/**7**)	**330** **(8)**	318/**331** (18/**4**)	**335** **(8)**	328/**333** (11/**7**)		334/**345** **(17/7)**	
0304	313/**322** (11/**5**)	**309** **(9)**	319/**329** (14/**5**)	**332** **(8)**	332/**337** (8/**5**)		338/**345** (11/**5**)	
0405	303/**308** (9/**4**)	**314** **(6)**	313/**322** (13/**3**)	**325** **(8)**	321/**323** (6/**4**)	316/**322** (9/**8**)	331/**338** (12/**4**)	315/**319** (9/**8**)
0506	309/**314** (9/**4**)	**321** **(9)**	320/**332** (15/**4**)	**333** **(6)**	326/**330** (8/**4**)	319/**322** (11/**10**)	337/**344** (12/**4**)	327/**330** (10/**10**)
0607	312/**317** (9/**3**)	**325** **(6)**	310/**316** (9/**5**)	**324** **(5)**	331/**335** (7/**3**)	327/**332** (14/**7**)	328/**332** (8/**3**)	327/**331** (10/**9**)
0708	311/**316** (8/**3**)		318/**326** (10/**4**)		329/**333** (8/**4**)	325/**329** (13/**9**)	338/**343** (9/**4**)	328/**338** (16/**15**)
0809	320/**330** (13/**6**)		330/**342** (15/**6**)		334/ **340** (8/**4**)	323/**329** (12/**12**)	344/**352** (12/**3**)	328/**338** (14/**11**)
AVG	311/**318** (11/**4**)		318/**328** (11/**3**)		329/**333** (6/**4**)	322/**327** (12/**9**)	336/**343** (9/**4**)	325/**331** (12/**11**)

Table 7. Comparison of ice phenological parameters for break-up period (MO and Ice-Off) daily-derived from AMSR-E (AME), QuikSCAT (QUT) and NOAA/IMS (IMS) products for GBL and GSL (2002–2009). Values within confidence regions in bold. Standard deviation in parentheses.

Pixel Level	MO				Ice-Off					
	GBL		GSL		GBL			GSL		
YEAR	AME	QUT	AME	QUT	AME	QUT	IMS	AME	QUT	IMS
0203	133/**127** (14/**12**)	**117** **(8)**	132/**137** (14/**5**)	**112** **(5)**	193/**183** **(14/7)**	**189** **(6)**		172/**157** (19/**2**)	**163** **(6)**	
0304	156/**155** (3/**2**)	**149** **(2)**	147/**150** (16/**6**)	**143** **(8)**	203/**198** (7/**4**)	**205** **(3)**	202/**204** (8/**6**)	186/**169** (20/**4**)	**178** **(5)**	176/**174** (17/**14**)
0405	133/**132** (11/**7**)	**152** **(14)**	124/**131** (21/**17**)	**100** **(1)**	193/**186** (11/**4**)	**193** **(5)**	188/**188** (12/**7**)	168/**155** (19/**4**)	**164** **(7)**	166/**160** (12/**10**)
0506	129/**128** (7/**4**)	**127** **(10)**	119/**122** (9/**5**)	**118** **(16)**	182/**169** (16/**5**)	**174** **(5)**	171/**172** (12/**10**)	161/**140** (21/**6**)	**151** **(11)**	148/**145** (13/**10**)
0607	142/**141** (10/**6**)		124/**129** (17/**6**)		197/**187** (12/**6**)		187/**187** (13/**9**)	166/**153** (19/**5**)		159/**158** (14/**6**)
0708	149/**152** (9/**9**)		133/**135** (16/**10**)		187/**183** (10/**4**)		185/**188** (9/**7**)	170/**156** (20/**2**)		161/**159** (13/**5**)
0809	167/**168** (8/**7**)		135/**137** (18/**14**)		200/**197** (6/**3**)		198/**200** (12/**5**)	177/**167** (16/**3**)		175/**174** (19/**7**)
AVG	144/**143** (6/**3**)		131/**134** (12/**5**)		194/**186** (9/**3**)		189/**190** (11/**7**)	171/**157** (17/**3**)		164/**162** (15/**9**)

TCD
5, 3129–3173, 2011

Table 8. Comparison of daily-derived ICDp from AMSR-E (AME), QuikSCAT (QUT) and NOAA/IMS (IMS) products for GBL and GSL (2002–2009). Values within confidence regions in bold. Standard deviation in parentheses. Note that QUT* indicates that ICDp was calculated from FO to ice-off since ice-on was not determined in Howell et al. (2009)

Pixel Level	ICDp					
	GBL			GSL		
YEAR	AME	QUT*	IMS	AME	QUT*	IMS
0203	224/**215** (19/**11**)	**224 (13)**		195/**220** (28/**29**)	**193 (12)**	
0304	233/**226** (12/**7**)	**260 (11)**		203/**223** **(22/22)**	**211 (12)**	
0405	232/**229** (10/**7**)	**245 (9)**	238/**232** (11/**7.5**)	195/**218** (20/**22**)	**205 (14)**	217/**207** (11/9)
0506	210/**203** (15/**7**)	**218 (13)**	217/**216** (12/**10**)	176/**201** **(26/26)**	**183 (16)**	186/**181** (12/10)
0607	225/**217** (14/**8**)		225/**221** (14/**8**)	195/**214** (17/**21**)		197/**193** (12/7.5)
0708	219/**215** (10/**6**)		225/**225** (11/**8**)	184/**193** (12/**14**)		198/**187** (15/10)
0809	230/**223** (11/**5**)		241/**237** (12/**8.5**)	193/**208** (18/**19**)		213/**202** (17/9)
AVG	225/**218** (9/**6**)		229/**226** (12/**8.3**)	192/**211** (16/**18**)		202/**194** (13/9.6)

TCD
5, 3129–3173, 2011

Table 9. Comparison of ice phenological parameters (CFO, WCI, and ICDe) daily derived from AMSR-E (AME) and NOAA/IMS (IMS) products, as well as weekly-derived from Canada Ice Service (CIS) product for GBL and GSL (2002–2009). Values within confidence regions in bold. Standard deviation in parentheses.

Entire Lake	CFO						WCI						ICDe					
	GBL			GSL			GBL			GSL			GBL			GSL		
YEAR	AME	IMS	CIS	AME	IMS	CIS	AME	IMS	CIS	AME	IMS	CIS	AME	IMS	CIS	AME	IMS	CIS
0203	346/ **346**		354	351/ **351**		354	210/ **210**		199	210 / **160**		178	229/ **229**		203	224/ **174**		182
0304	344/ **344**		339	350/ **350**		346	210/ **210**	208	219	210/ **194**	202	198	231/ **231**		238	225/ **209**		210
0405	330/ **330**	326	324	344/ **344**	326	338	210/ **210**	209	203	210/ **166**	186	196	246/ **246**	249	237	232/ **188**	226	216
0506	336/ **336**	334	336	349/ **349**	340	343	210/ **202**	187	188	207/ **168**	183	165	239/ **231**	218	210	223/ **184**	208	182
0607	339/ **339**	336	335	337/ **337**	337	335	210/ **208**	202	201	210/ **164**	175	187	236/ **234**	231	224	238/ **192**	203	210
0708	339/ **339**	345	341	346/ **346**	342	341	210/ **193**	195	200	210/ **158**	189	200	236/ **219**	215	217	230 / **178**	212	217
0809	348/ **348**	331	333	356/ **356**	348	347	210/ **204**	208	212	210/ **172**	199	191	228/ **222**	243	237	219/ **181**	217	202
AVG	340/ **340** (6/**6**)	334 (7)	337 (9)	348/ **347** (6/**6**)	339 (8)	343 (6)	210/ **203** (0/**6**)	202 (9)	203 (10)	210/ **164** (1/**11**)	189 (10)	188 (13)	234/ **230** (6/**9**)	231 (15)	224 (14)	227/ **187** (6/**12**)	213 (9)	203 (15)

TCD
5, 3129–3173, 2011
Estimating ice phenology on large northern lakes from AMSR-E
K.-K. Kang et al.

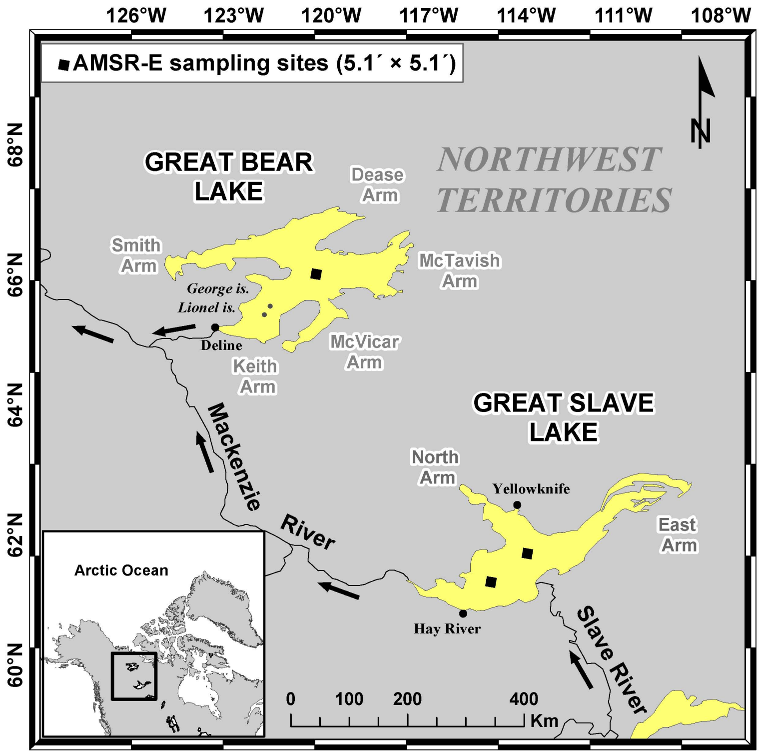

Fig. 1. Map showing location of Great Bear Lake (GBL) and Great Slave Lake (GSL), and their meteorological stations (Deline, Yellowknife, and Hay River) within the Mackenzie River Basin. Solid squares represent 5.1′ × 5.1′ of sampling sites at 18.7 GHz for the development of the ice phenological algorithm.

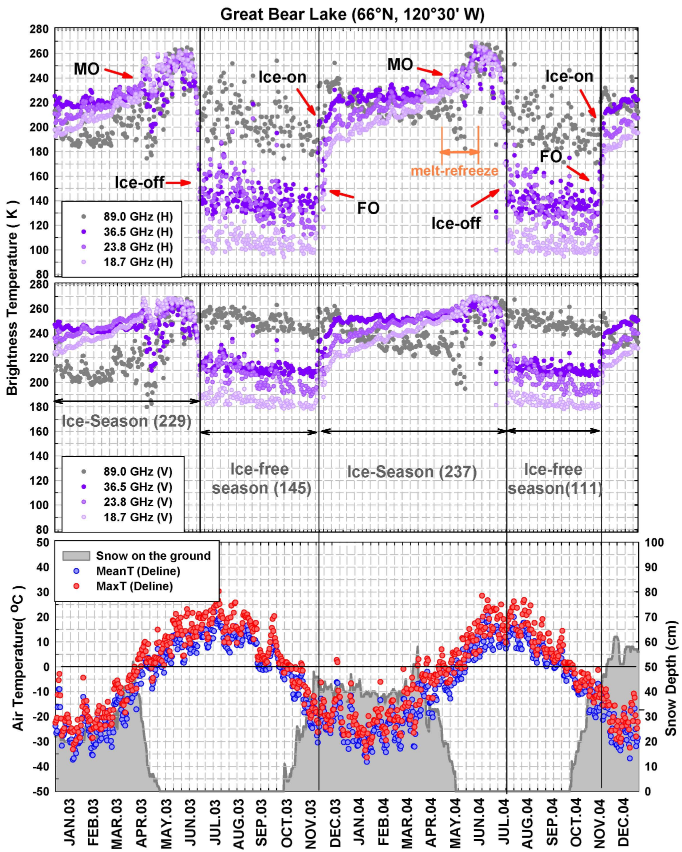

Fig. 2. Temporal evolution of horizontal (top) and vertical (middle) polarized brightness temperature at 18.7 (light violet), 23.8 (middle violet), 36.5 (dark violet), 89.0 (dark grey) GHz (2003–2004) for sampling site on GBL (see Fig. 1). The time series of maximum (Max_T, red) and mean ($Mean_T$, blue) air temperatures obtained at Deline meteorological station is shown in the bottom panel of the figure, with snow depth as grey shaded area.

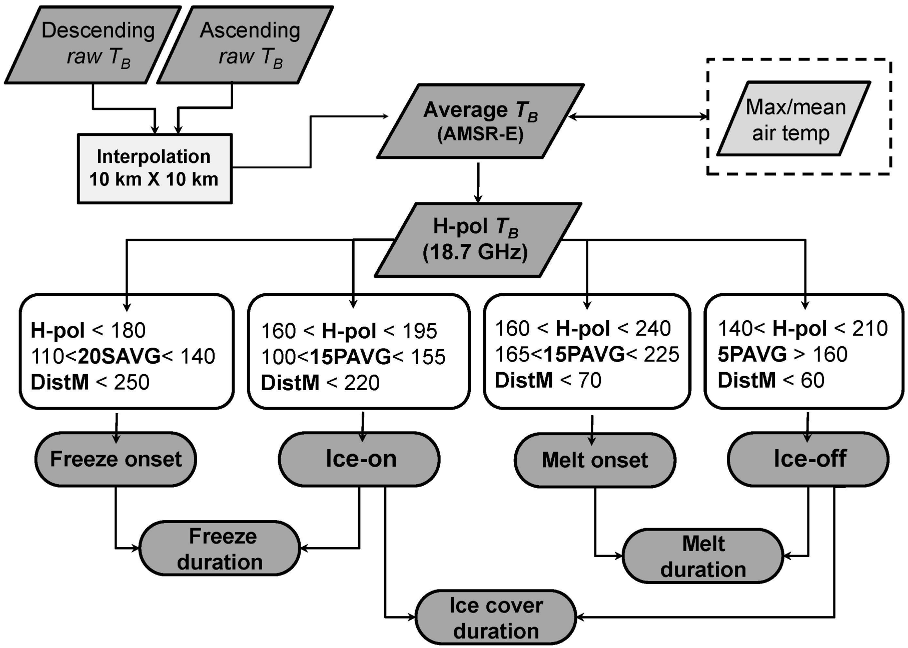

Fig. 3. Flowchart of ice phenology algorithm based on AMSR-E 18.7 GHz horizontal polarization (H-pol) brightness temperature (T_B). All threshold values are explained in Sect. 5.3.

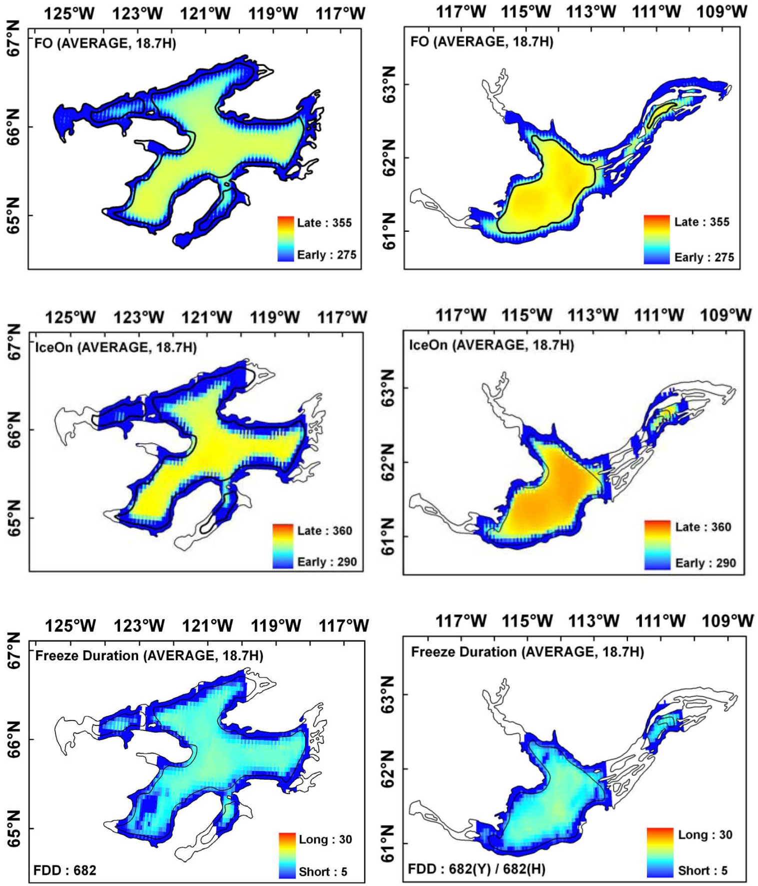

Fig. 4. Freeze-onset (FO), ice-on, and freeze-duration on average (2002–2009) for GBL (left panel) and GSL (right panel). Legend is day of year.

TCD
5, 3129–3173, 2011

Estimating ice phenology on large northern lakes from AMSR-E

K.-K. Kang et al.

Title Page
Abstract Introduction
Conclusions References
Tables Figures
◀ ▶
Back Close
Full Screen / Esc
Printer-friendly Version
Interactive Discussion

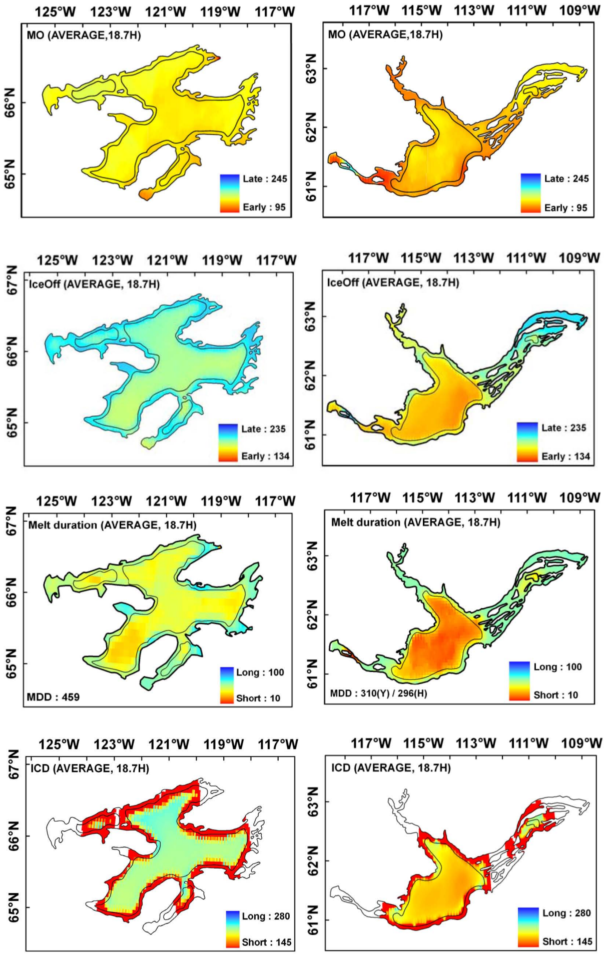

Fig. 5. Melt-onset (MO), ice-off, melt-duration, and ice-cover-duration (ICD) on average (2002–2009) for GBL (left panel) and GSL (right panel). Legend is day of year.

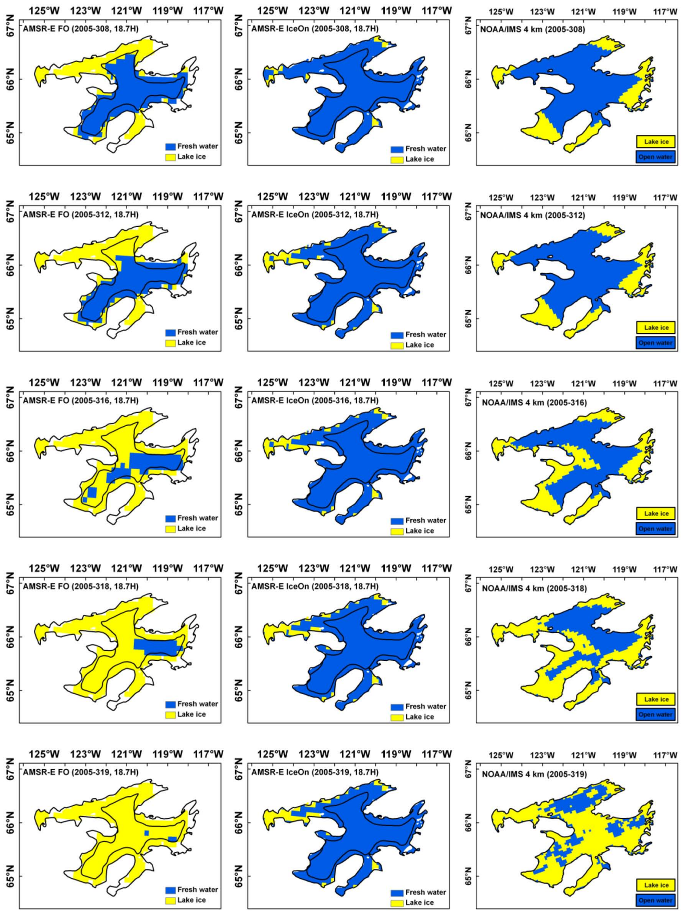

Fig. 6. Comparison of AMSR-E freeze-onset (left), ice-on (center), and NOAA/IMS ice-on (right) (day of year) during the freeze-up period of ice season 2005–2006 on GBL.

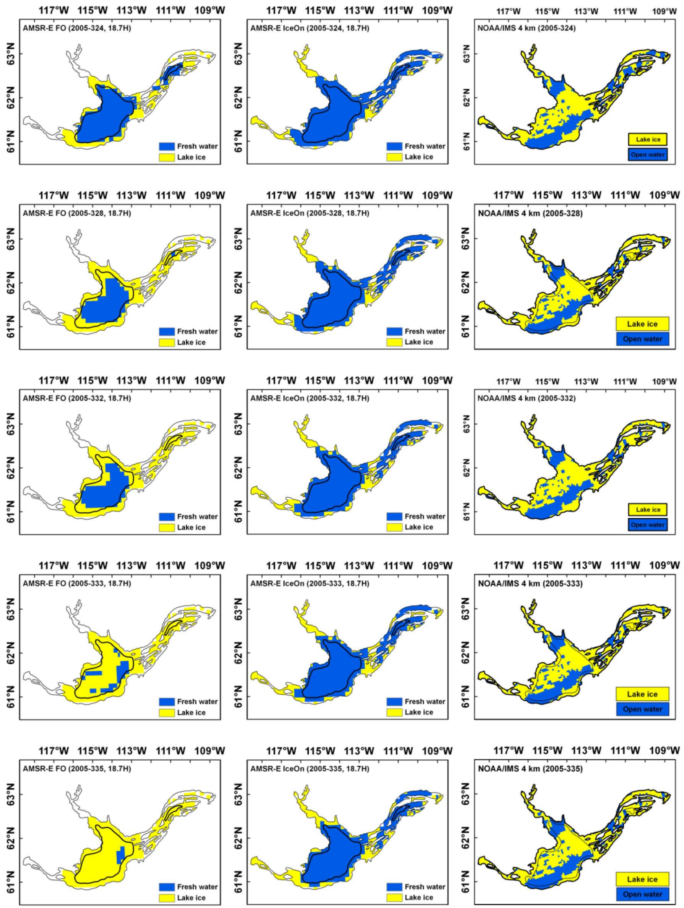

Fig. 7. Comparison of AMSR-E freeze-onset (left), ice-on (center), and NOAA/IMS ice-on (right) (day of year) during the freeze-up period of ice season 2005–2006 on GSL.

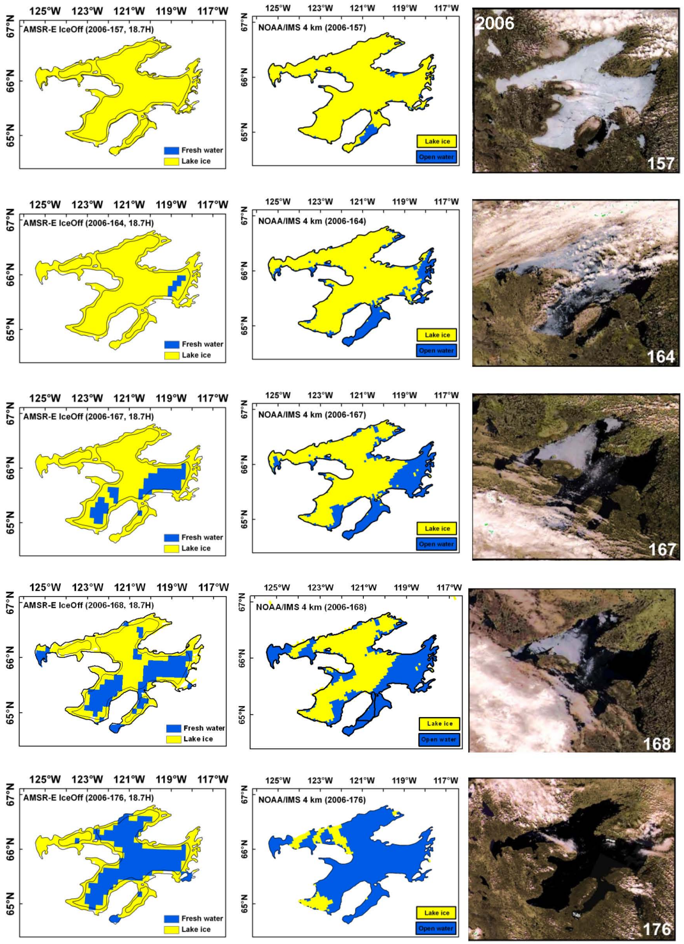

Fig. 8. Comparison of AMSR-E (left) and NOAA/IMS (center) ice-off, and MODIS/Terra image (right) acquired on the same day during the break-up period of ice season 2005–2006 on GBL.

TCD

5, 3129–3173, 2011

Estimating ice phenology on large northern lakes from AMSR-E

K.-K. Kang et al.

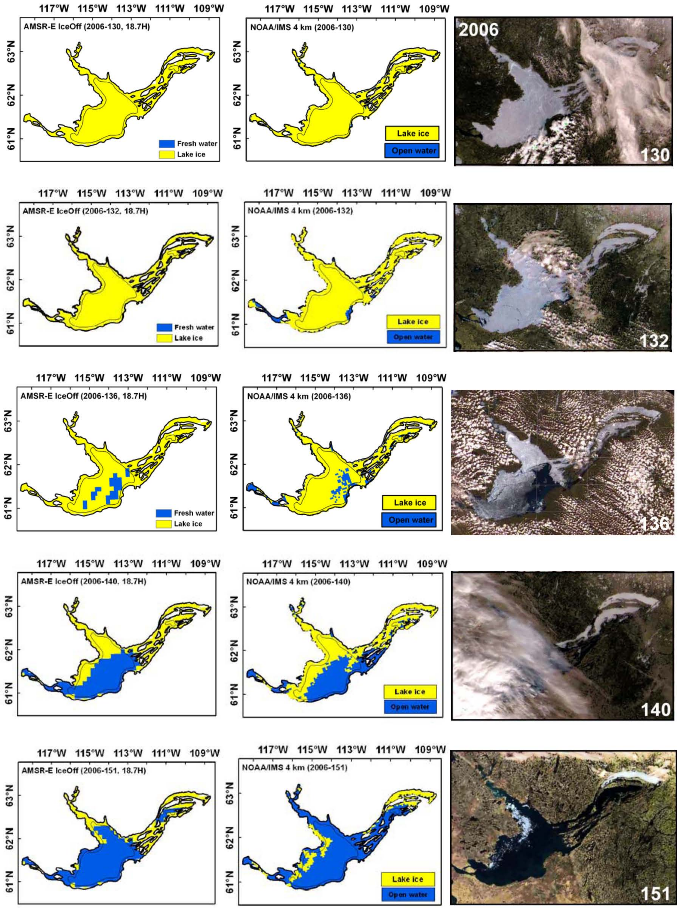

Fig. 9. Comparison of AMSR-E (left) and NOAA/IMS (center) ice-off, and MODIS/Terra image (right) acquired on the same day during the break-up period of ice season 2005–2006 on GSL.